

Basic Study

Jianpi Gushen Huayu decoction ameliorated diabetic nephropathy through modulating metabolites in kidney, and inhibiting TLR4/NF- κ B/NLRP3 and JNK/P38 pathways

Zi-Ang Ma, Li-Xin Wang, Hui Zhang, Han-Zhou Li, Li Dong, Qing-Hai Wang, Yuan-Song Wang, Bao-Chao Pan, Shu-Fang Zhang, Huan-Tian Cui, Shu-Quan Lv

Specialty type: Endocrinology and metabolism

Provenance and peer review: Unsolicited article; Externally peer reviewed.

Peer-review model: Single blind

Peer-review report's scientific quality classification

Grade A (Excellent): 0
Grade B (Very good): B, B
Grade C (Good): 0
Grade D (Fair): D
Grade E (Poor): 0

P-Reviewer: Cai L, United States; Kotlyarov S, Russia; Mao XM, China

Received: September 24, 2023

Peer-review started: September 24, 2023

First decision: November 30, 2023

Revised: December 21, 2023

Accepted: January 30, 2024

Article in press: January 30, 2024

Published online: March 15, 2024



Zi-Ang Ma, Graduate School, Hebei University of Chinese Medicine, Shijiazhuang 050000, Hebei Province, China

Li-Xin Wang, Hui Zhang, Li Dong, Qing-Hai Wang, Yuan-Song Wang, Bao-Chao Pan, Shu-Fang Zhang, Department of Endocrinology, Cangzhou Hospital of Integrated Traditional Chinese Medicine and Western Medicine of Hebei Province Affiliated to Hebei University of Chinese Medicine, Cangzhou 061000, Hebei Province, China

Han-Zhou Li, School of Integrative Medicine, Tianjin University of Traditional Chinese Medicine, Tianjin 300000, China

Huan-Tian Cui, The First School of Clinical Medicine, Yunnan University of Traditional Chinese Medicine, Kunming 065000, Yunnan Province, China

Shu-Quan Lv, Department of Endocrinology, Hebei Cangzhou Hospital of Integrative Medicine, Cangzhou 061000, Hebei Province, China

Corresponding author: Shu-Quan Lv, Doctor, Chief Physician, Department of Endocrinology, Hebei Cangzhou Hospital of Integrative Medicine, No. 31 Huanghe Road, Cangzhou 061000, Hebei Province, China. czlvshuquan@163.com

Abstract

BACKGROUND

Jianpi Gushen Huayu Decoction (JPGS) has been used to clinically treat diabetic nephropathy (DN) for many years. However, the protective mechanism of JPGS in treating DN remains unclear.

AIM

To evaluate the therapeutic effects and the possible mechanism of JPGS on DN.

METHODS

We first evaluated the therapeutic potential of JPGS on a DN mouse model. We then investigated the effect of JPGS on the renal metabolite levels of DN mice using non-targeted metabolomics. Furthermore, we examined the effects of JPGS on c-Jun N-terminal kinase (JNK)/P38-mediated apoptosis and the inflammatory

responses mediated by toll-like receptor 4 (TLR4)/nuclear factor-kappa B (NF- κ B)/NOD-like receptor family pyrin domain containing 3 (NLRP3).

RESULTS

The ameliorative effects of JPGS on DN mice included the alleviation of renal injury and the control of inflammation and oxidative stress. Untargeted metabolomic analysis revealed that JPGS altered the metabolites of the kidneys in DN mice. A total of 51 differential metabolites were screened. Pathway analysis results indicated that nine pathways significantly changed between the control and model groups, while six pathways significantly altered between the model and JPGS groups. Pathways related to cysteine and methionine metabolism; alanine, tryptophan metabolism; aspartate and glutamate metabolism; and riboflavin metabolism were identified as the key pathways through which JPGS affects DN. Further experimental validation showed that JPGS treatment reduced the expression of TLR4/NF- κ B/NLRP3 pathways and JNK/P38 pathway-mediated apoptosis related factors.

CONCLUSION

JPGS could markedly treat mice with streptozotocin (STZ)-induced DN, which is possibly related to the regulation of several metabolic pathways found in kidneys. Furthermore, JPGS could improve kidney inflammatory responses and ameliorate kidney injuries in DN mice *via* the TLR4/NF- κ B/NLRP3 pathway and inhibit JNK/P38 pathway-mediated apoptosis in DN mice.

Key Words: Diabetic nephropathy; Jianpi Gushen Huayu Decoction; Oxidative stress; Inflammation; Untargeted metabolomics; Toll-like receptor 4/nuclear factor-kappa B/NOD-like receptor family pyrin domain containing 3 pathway; c-Jun N-terminal kinase/P38-mediated apoptosis

©The Author(s) 2024. Published by Baishideng Publishing Group Inc. All rights reserved.

Core Tip: Traditional Chinese medicine (TCM) has been demonstrated to possess beneficial effects on diabetes and its complications. Elucidating upon these mechanisms can contribute to the modernization of TCM. The dysfunction of metabolism is closely related to the progression of diabetes and diabetic complications. Using untargeted metabolomics can be useful in studying the metabolic regulatory mechanisms of TCM. The current study used untargeted metabolomics to evaluate the differential metabolites in a diabetic nephropathy (DN) mouse model after Jianpi Gushen Huayu Decoction (JPGS) treatment. Moreover, we deeply analyzed the results from metabolomics and tested the potential pathways related to the differential metabolites. Our results revealed that JPGS could markedly treat mice with streptozotocin (STZ)-induced DN. The metabolomics results exhibited that the efficacy of JPGS is possibly related to cysteine and methionine metabolism; alanine, aspartate, and glutamate metabolism; tryptophan metabolism; and riboflavin metabolism.

Citation: Ma ZA, Wang LX, Zhang H, Li HZ, Dong L, Wang QH, Wang YS, Pan BC, Zhang SF, Cui HT, Lv SQ. Jianpi Gushen Huayu decoction ameliorated diabetic nephropathy through modulating metabolites in kidney, and inhibiting TLR4/NF- κ B/NLRP3 and JNK/P38 pathways. *World J Diabetes* 2024; 15(3): 502-518

URL: <https://www.wjgnet.com/1948-9358/full/v15/i3/502.htm>

DOI: <https://dx.doi.org/10.4239/wjd.v15.i3.502>

INTRODUCTION

As a frequent complication of type 2 diabetes mellitus (T2DM), diabetic nephropathy (DN) is insidious and highly prevalent. In the early stages, DN progresses slowly and is reversible; however, in later stages it progresses rapidly and confers an unfavorable prognosis[1]. Conventional treatments of DN include controlling blood glucose levels, reducing blood pressure, and improving microcirculation[2]. The above treatments using Western drugs (*e.g.*, antihypertensives) can prevent DN to a certain extent, however, they exert negligible effects on patients with advanced DN[3]. Therefore, developing safe and reliable agents to cut off or delay the progression of DN has become a well-explored area of research.

Traditional Chinese medicine (TCM) is markedly efficacious in improving the clinical symptoms of DM and delaying its progression[4]. A study speculated that quercetin may be used to treat T2DM by targeting the transduction of mitogen-activated protein kinase (MAPK) pathways[5], and that crocin may be used to treat DM by inducing insulin sensitivity, improving insulin signal transduction, and preventing pancreatic β cell failure[6]. Huanglian Jiedu Decoction may be used to treat T2DM and its complications by synergistically regulating and participating in multiple biological processes (*e.g.*, signal transduction, inflammatory responses, and apoptotic and vascular processes) and pathways[7].

Metabolomics is commonly used in understanding both the interactions between metabolites and pathological conditions and the changes to metabolic profiles during drug interventions[8]. A study wherein the early DN rat sera were quantitatively measured by metabolomics suggested that guanosine, oleic acid, and glutamate may be potential biomarkers of kidney injury[9]. Furthermore, *Scutellaria baicalensis* and *Coptis chinensis* regulated the contents of

trihydroxytrimethyloxindole, leukotrienes, leucylproline, and estradiol in the feces of T2DM rats and primarily interfered with the metabolism of sphingolipids and fatty acids[10-12]. Regulating metabolism to ameliorate DN has recently become a well-explored research area[13]. In another study, metabolomic analysis revealed that the lipid metabolites were improved in the sera of DM mice treated with *Rehmannia glutinosa* and *Coptis chinensis* as compared to that of model mice[14]. Moreover, when the kidney tissue samples of rats were analyzed by metabolomics, orally administered astragaloside IV could protect the kidneys by improving region-specific metabolic disorders[15].

Jianpi Gushen Huayu Decoction (JPGS) - consisting of *Astragalus membranaceus*, *Panax ginseng*, *Comus officinalis*, *Dioscorea opposita*, *Gordon Euryale* seeds, *Rosa laevigata*, *Atractylodes macrocephala*, *Angelica sinensis*, *Salvia miltiorrhiza*, *Rhizoma Chuanxiong*, *Whitmania pigra* Whitman, and *Rhei Radix et Rhizoma* is clinically highly efficacious on DN[16]; nevertheless, its reno-protective mechanism of action on DN remains uninvestigated. In this study, we investigated the therapeutic effect of JPGS in a DN mouse model. We then examined the effect of JPGS on the levels of renal endogenous metabolites by using non-targeted metabolomics. Furthermore, we examined the effects of JPGS on c-Jun N-terminal kinase (JNK)/P38-mediated apoptosis and inflammatory responses as mediated by the toll-like receptor 4 (TLR4)/nuclear factor-kappa B (NF- κ B)/NOD-like receptor family pyrin domain containing 3 (NLRP3).

MATERIALS AND METHODS

Animals and materials

Sixty healthy male C57BL/6 mice (with an average body weight of 21 ± 1 g) were obtained from Beijing Huafukang Co., Ltd. Each cage which was maintained at a room temperature of 20-23 °C and at relative humidity levels of 50%-60% - housed five mice which were entrained to a 12 h/12 h light-dark cycle. The mice had free access to food and water. The animal study was reviewed and approved by Ethics Committee of Hebei University of Chinese Medicine (Approval No. CZX2021-KY-026). Details of the materials and reagents employed in this study were shown in Supplementary material.

Preparation of JPGS

In accordance with the JPGS prescription, the following quantities of single extract of Chinese traditional medicinal crops were weighed: 7 g of *Astragalus membranaceus*, 2.1 g of *Panax ginseng*, 4.4 g of *Comus officinalis*, 1.8 g of *Dioscorea opposita*, 0.7 g of *Gordon Euryale* seeds, 2.4 g of *Rosa laevigata*, 4.1 g of *Atractylodes macrocephala*, 3.5 g of *Angelica sinensis*, 2.6 g of *Salvia miltiorrhiza*, 1.8 g of *Rhizoma Chuanxiong*, 0.4 g of *Whitmania pigra* Whitman, and 1.2 g of *Rhei Radix et Rhizoma*. The TCM prescription dispensing machine (ARTEMIS-M540, EFong Pharmaceutical, Guangdong, China) was used to combine the above extracts into a single bag for further use. Subsequently, the mixed extracts were dissolved with water, and the concentration was controlled to 5.3 g/mL. The mixture was stored at 4 °C. Ultra performance liquid chromatography coupled with mass spectrometer was conducted as the quality control of JPGS, as detailed in the Supplementary material. Total ion chromatogram and chromatography of JPGS were shown in [Supplementary Figure 1](#) and [Supplementary Table 1](#).

Animal experiments

All mice underwent one-week adaptive feeding before receiving a high-sugar and high-fat diet (HFD) containing 34% sucrose, 21% fat, 0.15% cholesterol, and 44.85% conventional treats for eight weeks. After eight weeks of HFD feeding, the mice were modeled as follows: All mice underwent fasting for 12 h with unrestricted access to water and were then intraperitoneally treated with 30 mg/kg streptozotocin (STZ), except for the mice in the control group, which were intraperitoneally administrated with an equal volume of the vehicle. Seventy-two hours following STZ administration, blood from the tail vein was collected from the mice to perform fasting blood glucose (FBG) tests, and mice with a FBG ≥ 12.0 mmol/L were confirmed as having T2DM. The mice were then fed with HFD continuously and tested weekly for 24 h urine total protein (24 h-UTP). Successful DN modeling was identified based on the criteria of a FBG ≥ 12.0 mmol/L and a 24 h-UTP ≥ 20 mg.

After modeling; the mice were divided into the model, irbesartan (IRBE), low-dose JPGS (JPGSL), medium-dose JPGS (JPGSM), and high-dose JPGS (JPGSH) groups according to the random number table, with ten mice assigned to each group. The mice, in the control and model groups received 0.2 mL of normal saline; in the IRBE group received 30 mg/kg/d IRBE; and in the JPGSL, JPGSM, and JPGSH groups received 2.4, 4.8, and 9.6 g/kg/d, *via* gavages, respectively. The duration of administration in each group was four consecutive weeks, and FBG levels and body weight were measured weekly. After four weeks of JPGS treatment, 24 h urinary samples of the mice in each group were collected in metabolic cages. In addition, blood samples were collected *via* the inner canthus. After the mice were euthanized, the abdominal cavity was opened; the left kidneys were collected and immobilized in a 4% paraformaldehyde solution, whereas the right kidneys were cryopreserved.

Measurement of kidney function, oxidative stress, and inflammation-related parameters

The collected 24 h urinary samples were centrifuged ($4000 \times g$, 10 min) to obtain the supernatant. 24 h-UTP was measured according to the kit instructions. Blood samples were centrifuged ($400 \times g$, 15 min) to prepare serum, while the creatinine (Cr) and blood urea nitrogen (BUN) levels in sera were measured according to the kit instructions. Frozen kidney tissue samples and normal saline were mixed at a 1:9 ratio, the resulting mixture was homogenized and centrifuged ($400 \times g$, 15 min), and the supernatant was prepared for the kidney tissue homogenate. The activities of superoxide dismutase (SOD), glutathione peroxidase (GSH-Px), and the level of malondialdehyde (MDA) in the kidney tissue homogenates were

measured according to the kit instructions; the levels of interleukin (IL)-6, IL-1 β , and tumor necrosis factor alpha (TNF- α) in the kidney tissue homogenates in each group were detected by enzyme-linked immunosorbent assay. Meanwhile, total protein concentrations in kidney tissue homogenates were tested to homogenize the samples.

Hematoxylin and eosin, periodic acid Schiff, and TUNEL staining

Kidneys immobilized in a 4% paraformaldehyde solution were dehydrated, embedded in paraffin, and sliced into 4 μ m-thick sections, which sequentially underwent hematoxylin and eosin (HE), periodic acid Schiff (PAS), and TUNEL staining. The dehydrated and mounted sections were then microscopically observed. Quantification of HE staining was conducted according to the severity of tubular dilatation, brush border loss, tubular necrosis, and cast formation as established in a previous study[17]. Moreover, the glomerulosclerosis index was used to assess the severity of glomerulosclerosis in PAS staining[18]. Apoptosis was observed using TUNEL staining, and TUNEL staining-positive regions were measured by Image J (version 1.52a, NIH, Bethesda, MD, United States).

Non-targeted metabolomics analysis

A total of 100 mg of frozen kidney tissue was finely ground in liquid nitrogen, placed into a 1.5 mL tube with 500 μ L of 80% methanol; the tube was then vortexed, oscillated, and cooled. Further, the mixture was centrifuged (15000 \times g, 20 min). The supernatant was obtained and diluted with ultrapure water to a volume containing 53% methanol, which was centrifuged at 15000 \times g at 4 $^{\circ}$ C for 20 min to remove the supernatant. An aliquot (20 μ L) of each sample was obtained; all the aliquots were subsequently mixed well. The resulting mixture was taken as the quality control sample. See Supplementary material for details of liquid chromatography-mass spectrometry conditions, gradient elution program (Supplementary Table 2) and data acquisition, processing, and steps taken in conducting the analysis.

Western blotting

Approximately 30 mg of frozen kidney tissue was weighed so as to extract the total protein available. The concentrations of the protein samples were then investigated, and a loading buffer was mixed with protein samples, which underwent denaturation *via* incubation at 97 $^{\circ}$ C for 5 min. The protein samples were separated using sodium-dodecyl sulfate gel electrophoresis and transferred onto a 0.22 μ m polyvinylidene fluoride membrane using the wet transfer method. After 2 h blocking in 5% skim milk, TLR4, P65, phosphorylated P65 (p-P65), NLRP3, cleaved-caspase-1, caspase-1, protein apoptosis-associated speck-like protein containing a CARD (ASC), IL-1 β , IL-18, phosphorylated JNK (p-JNK), JNK, phosphorylated p38 (p-P38), P38, caspase-3, caspase-9, and β -actin were added respectively for the primary antibody incubation at 4 $^{\circ}$ C overnight. Further, the membranes were washed and the corresponding secondary antibodies, diluted at a volume ratio of 1:4000, were added and incubated for 2 h at room temperature. The membranes were then washed thrice. After adding an enhanced chemiluminescence developer for a complete reaction; the membranes were exposed to a stand-alone gel imaging system so as to reveal the protein bands. ImageJ software was utilized to measure the grey values of various bands and to quantify the relative expression of the proteins.

Reverse transcription-quantitative polymerase chain reaction

Total RNA was extracted from the kidney tissue using Trizol reagent, followed by reverse transcription into cDNA using a kit. Gene expression was analyzed using a reverse transcription-quantitative polymerase chain reaction (RT-qPCR) detection system and a SuperReal PreMix Plus kit. At the messenger ribonucleic acid (mRNA) level, the expression quantity of target genes relative to the housekeeping gene *Actb* was calculated *via* the $2^{-\Delta\Delta CT}$ method. Primer sequences were shown in Supplementary Table 3.

Statistical methods

SPSS Statistics 20.0 was used for data analysis. All data were presented as mean \pm SD. A one-way analysis of variance was conducted for multi-group comparisons and Tukey's honest significance difference test was used for *post-hoc* analysis, while the inter-group pairwise comparisons were conducted using a two-tailed Student's *t*-test. Analysis results with a *P* value < 0.05 were considered statistically significant.

RESULTS

Ameliorative effects of JPGS in a DN mouse model

During the four-week treatment period, alterations in the body weight and FBG levels were dynamically recorded on a weekly basis. After JPGS administration, body weight decreased significantly, and the FBG levels increased remarkably in DN mice compared to that of the normal mice. The mice's body weight increased and the FBG levels decreased notably in the IRBE, JPGSL, JPGSM, and JPGSH groups in comparison with that of the mice in the model group (Figure 1A and B). The kidney function test results revealed that the Cr and BUN levels and 24 h-UTP increased considerably in the mouse sera in the model group than that those of the control group. Furthermore, the Cr level markedly reduced in the IRBE, JPGSL, JPGSM, and JPGSH groups. The BUN level and 24 h-UTP decreased notably in the IRBE and JPGSH groups when compared to that of the model group (Figure 1C-E). The HE and PAS staining results showed that severe pathological changes (*e.g.*, glomerular hypertrophy, hyperplasia of mesangial matrix, and thickened glomerular basement membrane) occurred in the kidneys in the model group and could be improved by IRBE and JPGS (Figure 2A-D).

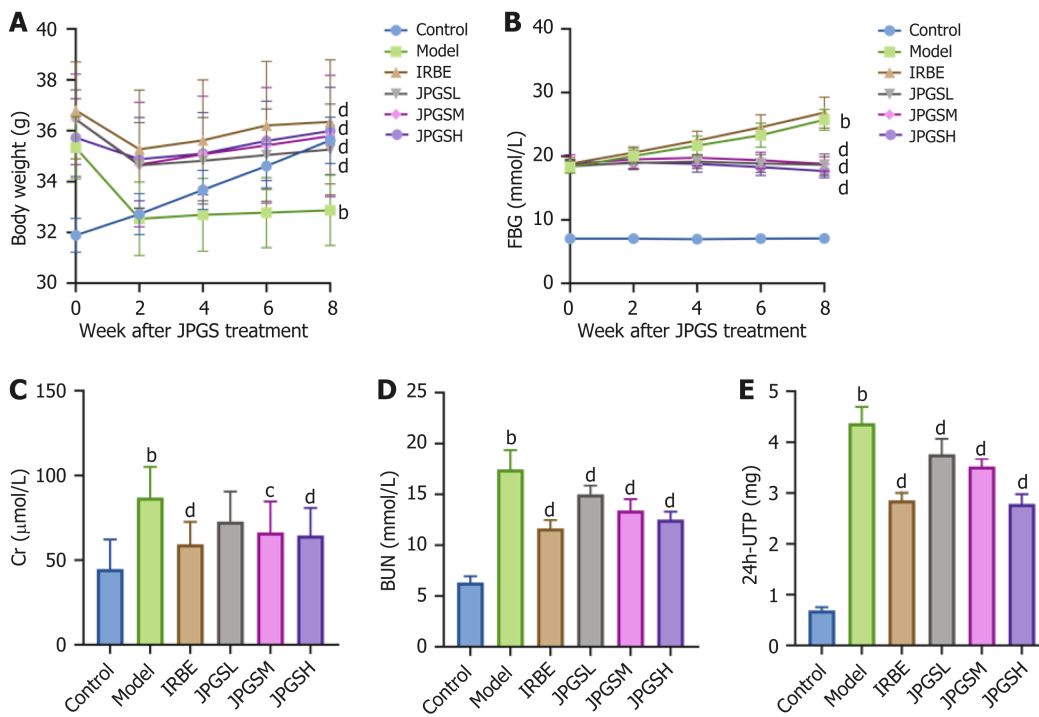


Figure 1 Jianpi Gushen Huayu Decoction administration improved body weight loss, hyperglycemia, and kidney injury in diabetic nephropathy mice. A: Curves of body weight changes; B: Curves of fasting blood glucose changes; C: Creatinine levels; D: Blood urea nitrogen level; E: 24 h urine total protein levels. Control, model, irbesartan, low-dose Jianpi Gushen Huayu Decoction (JPGSL), medium-dose JPGS, and high-dose JPGS groups, $n = 10$ per group. ^b $P < 0.01$ as compared to the control group; ^c $P < 0.05$ as compared to the model group; ^d $P < 0.01$ as compared to the model group. JPGS: Jianpi Gushen Huayu Decoction; FBG: Fasting blood glucose; Cr: Creatinine; BUN: Blood urea nitrogen; 24h-UTP: 24 h urine total protein; JPGSL: Low-dose Jianpi Gushen Huayu Decoction; JPGSM: Medium-dose Jianpi Gushen Huayu Decoction; JPGSH: High-dose Jianpi Gushen Huayu Decoction; IRBE: Irbesartan.

Changes in oxidative stress and inflammatory factor levels in DN mice following JPGS treatment

The activities of anti-oxidative enzymes (SOD, GSH-Px) decreased substantially, whereas the MDA level (a product of lipid peroxidation) notably increased in the model group in comparison to the control group, suggesting that oxidative stress was exacerbated in the kidney tissue of DN mice. The SOD and GSH-Px levels were markedly elevated and the MDA level decreased dramatically in IRBE, JPGSL, JPGSM, and JPGSH groups when compared to that of the model group, indicating that JPGS could notably alleviate oxidative stress in DN mice (Figure 3A-C).

The IL-6, IL-1 β , and TNF- α levels increased significantly in the model group compared to those of the control group and decreased noticeably in the IRBE, JPGSL, JPGSM, and JPGSH groups when compared to those of the model group, demonstrating that JPGS can notably reduce the inflammatory levels observed in the kidneys of DN mice (Figure 3D-F).

Effects of JPGS on metabolites in kidney tissues of DN mice

When examining the effects of JPGS on treating DN and improving oxidative stress, JPGSH had the highest improvement effect in DN mice. Therefore; control, model, and JPGSH groups were selected in this study to conduct metabolomics analyses. The principal component analysis results showed that the distributed clusters were markedly separated, signaling that the DN mice in the model group were successfully modeled, and that JPGS could considerably improve DN-associated kidney metabolite abnormalities in DN mice (Figure 4A). A predictive model was established by the partial least squares discriminant analysis (PLS-DA) and validated to further define inter-group differences. Based on a PLS-DA prediction model, we observed significant separation of the control and model groups, as well as the model and JPGSH groups, on the PLS-DA score maps with R²Y values in both cases being greater than 0.9, and Q² values being less than zero. This indicates that the model did not overfit and that the results carried a high degree of explanatory power (Figure 4B-E).

An ionic variable importance in projection score > 1 , $P < 0.05$, and a fold change > 2 or < 0.5 were the screening criteria for differential metabolites. A total of 51 differential metabolites were screened out from the control, model, and JPGSH groups (Table 1). The screened differential metabolites were introduced into MetaboAnalyst for metabolic pathway analysis. A total of four metabolic pathways: (1) Cysteine and methionine metabolism; (2) Alanine, aspartate and glutamate metabolism; (3) Tryptophan metabolism; and (4) Riboflavin metabolism were enriched as the common pathways (Figure 4F and G).

Changes in the TLR4/NF- κ B/NLRP3 pathway in the kidney tissue of DN mice following JPGS treatment

Recent studies suggested that the tryptophan metabolite N-acetylserotonin (NAS) could inhibit inflammatory responses via the TLR4/NF- κ B/NLRP3 pathway[19]. Our findings revealed that JPGS could reduce the NAS level in kidney tissue. As such, we evaluated the effect of JPGS on the TLR4/NF- κ B/NLRP3 pathway. Specifically, we measured the levels of

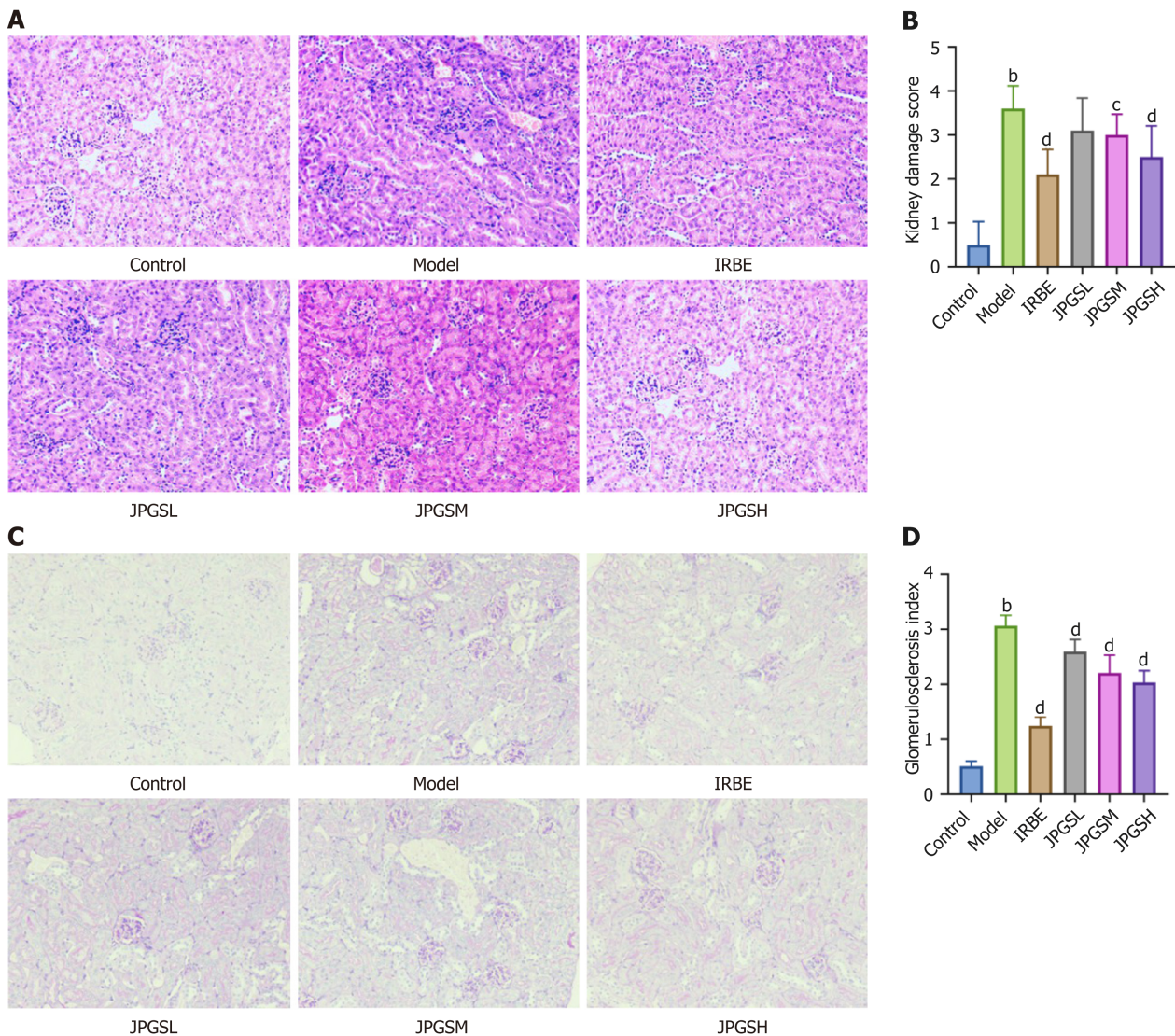


Figure 2 Pathological changes in kidneys were improved following Jianpi Gushen Huayu Decoction administration. A: Hematoxylin and eosin staining; B: Kidney damage score; C: Periodic acid Schiff staining; D: Glomerulosclerosis index, magnification $\times 100$. ^b $P < 0.01$ as compared to the control group; ^c $P < 0.05$ as compared to the model group; ^d $P < 0.01$ as compared to the model group. JPGSL: Low-dose Jianpi Gushen Huayu Decoction; JPGSM: Medium-dose Jianpi Gushen Huayu Decoction; JPGSH: High-dose Jianpi Gushen Huayu Decoction; IRBE: Irbesartan.

the critical proteins (*i.e.*, TLR4, p-P65/P65, NLRP3, ASC, cleaved caspase-1, mature IL-1 β , and IL-18) in the TLR4/NF- κ B/NLRP3 pathway using western blotting. The results signified that the expression levels of these critical proteins were notably elevated in the mouse kidneys in the model group compared to that of the control group, and decreased notably after treatment with JPGSH (Figure 5A-H).

Additionally, we measured the expression levels of *Nlrp3*, *Asc*, *casp1*, *IL1b*, and *Il18* in the TLR4/NF- κ B/NLRP3 pathway using quantitative RT-qPCR, with the results indicating that, at the mRNA level, the expression levels of *Nlrp3*, *Asc*, *casp1*, *IL1b*, and *Il18* increased notably in the mouse kidneys of the model group when compared to those of the control group and decreased significantly after treatment with JPGSH (Figure 5I-M).

Effect of JPGS on JNK/P38-mediated apoptosis in DN mice

A previous study has indicated that 5-hydroxyindole-3-acetic acid (5-HIAA), a tryptophan metabolite, could promote cell apoptosis *via* the JNK/P38 pathway[20]. The metabolomics results revealed that JPGS could reduce the 5-HIAA level. Therefore, we examined whether JPGS could affect JNK/P38 pathway-mediated apoptosis. Specifically, we observed the effect of JPGSH on apoptosis in DN mice using TUNEL staining; the results indicated that a massive amount of green fluorescence could be found in the kidney tissue of DN model mice, and positive fluorescence was markedly diminished in the kidney tissue of DN mice following JPGSH administration (Figure 6A and B).

Furthermore, we tested the levels of JNK phosphorylation, P38 phosphorylation, cleaved caspase-3, and cleaved caspase-9 in the JNK/P38 pathway; the results indicated that the degrees of p-JNK/JNK, p-P38/P38, cleaved caspase-3, and cleaved caspase-9 increased remarkably in the mouse kidneys of the model group when compared to those of normal mice and decreased dramatically after treatment with JPGSH (Figure 6C-G).

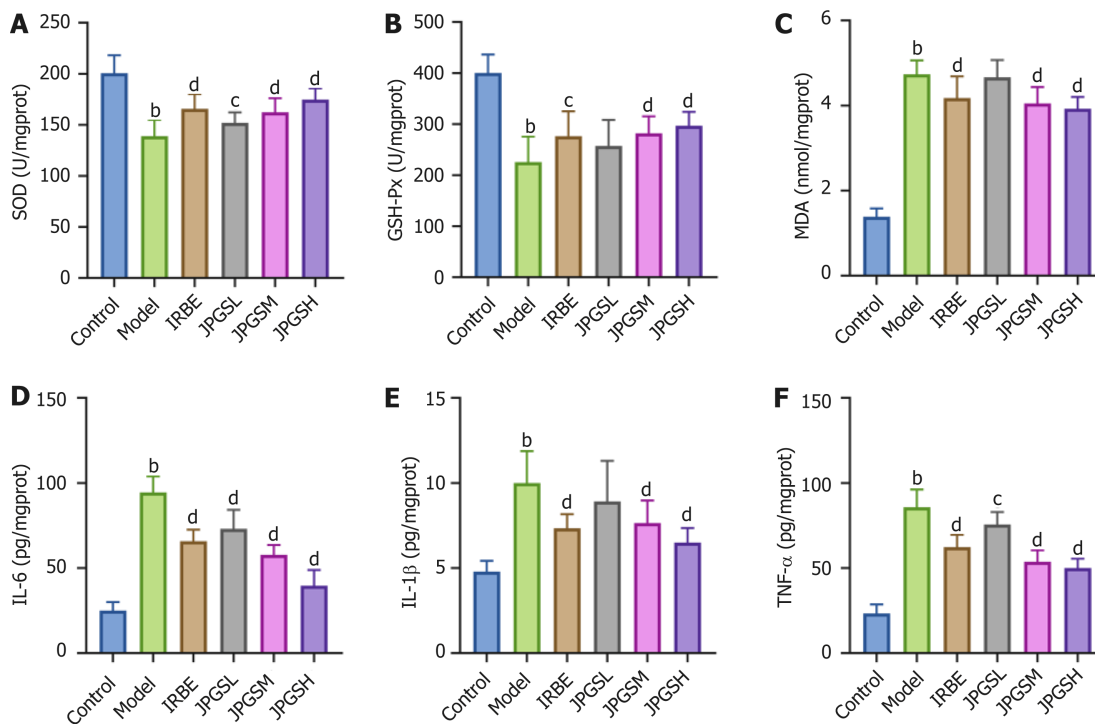


Figure 3 Jianpi Gushen Huayu Decoction reduced oxidative stress and inflammation in kidneys. A: The activities of superoxide dismutase; B: The activities of glutathione peroxidase; C: Malondialdehyde level; D: Interleukin (IL)-6 levels; E: IL-1 β levels; F: Tumor necrosis factor- α levels. ^a $P < 0.01$ as compared to the control group; ^b $P < 0.05$ as compared to the model group; ^d $P < 0.01$ as compared to the model group. JPGSL: Low-dose Jianpi Gushen Huayu Decoction; JPGSM: Medium-dose Jianpi Gushen Huayu Decoction; JPGSH: High-dose Jianpi Gushen Huayu Decoction; IRBE: Irbesartan; SOD: Superoxide dismutase; GSH-Px: Glutathione peroxidase; MDA: Malondialdehyde; IL-6: Interleukin 6; IL-1 β : Interleukin 1 beta; TNF- α : Tumor necrosis factor alpha.

DISCUSSION

JPGS, whose mechanism of action remains unknown, is commonly employed to treat DN in clinical practice[16]. In this study, we analyzed the effect of JPGS on the metabolism of DN mice and investigated the therapeutic effect of JPGS on DN and its underlying mechanism of action by using non-targeted metabolomics. The classic model mice with DN, as induced by HFD combined with STZ, could exhibit similar symptoms to those observed in patients with DN[21]. In this model, the mice were fed a high-sugar diet to induce insulin resistance and were injected with STZ to induce pancreatic β cell necrosis to trigger the loss of the insulin secretion function. As a result, persistent hyperglycemia led to kidney tubular atrophy, necrosis, and nephrotoxicity resulting in impaired kidney function and organic injury[22]. 24 h-UTP, which is the most sensitive parameter to assess early DN, is indicative of glomerular filtration impairment[23]. Cr and BUN levels, which are the major parameters used to assess kidney function, are generally utilized to estimate the glomerular filtration rate and an increase in the Cr and BUN levels in the serum signifies kidney dysfunction[24,25]. In this study, severe pathological changes (*e.g.*, glomerular and kidney tubular epithelial cell hypertrophy and thickened basement membrane), corresponding to the above symptoms occurred in the kidneys of DN mice and were effectively improved by JPGS. Moreover, IRBE is frequently employed to treat DN in clinical practice which was taken as the positive control in this study[26]. The findings revealed that JPGSH and IRBE were not significantly different in terms of efficacy. This suggested that JPGS could markedly treat DN; however, unveiling its mechanism of action which remains unknown requires further investigation.

Oxidative stress and inflammatory responses contribute considerably to the occurrence and progression of DN. Oxidative stress can induce inflammatory responses which, in turn, can exacerbate oxidative stress, while inflammation and oxidative stress can lead to alterations in kidney structure and function *via* multiple pathways[27]. In this study, JPGS exerted antioxidant and anti-inflammatory effects by helping to produce SOD and GSH-Px and reducing the MDA and proinflammatory cytokine contents. The exacerbation of oxidative stress is associated with an increase in the reactive oxygen species level, which correlates with endothelial dysfunction, changes in the extracellular matrix protein level, and an increase in kidney sodium reabsorption levels[28-30]. Exacerbated oxidative stress in DM patients could contribute to the occurrence of DN and cause DN to progress to end-stage kidney disease[31]. SOD and GSH-Px, which are major antioxidant enzymes, play a crucial role in maintaining the oxidant/antioxidant balance, whereas MDA is the lipid peroxidation end product in the body and its content is indicative of the degree of cellular oxidative injury[32]. IL-6, IL-1 β , and TNF- α , which are common inflammatory factors, play a vital role in inflammatory responses in the body[33]. Persistent hyperglycemia led to continuously elevated expression levels of inflammatory factors, resulting in exacerbated inflammatory responses[34].

The above studies on the efficacy of JPGS proved that it can effectively treat DN and that JPGSH had the greatest effect on improving DN. Thus, we selected the control, model, and JPGSH groups to investigate potential therapeutic pathways

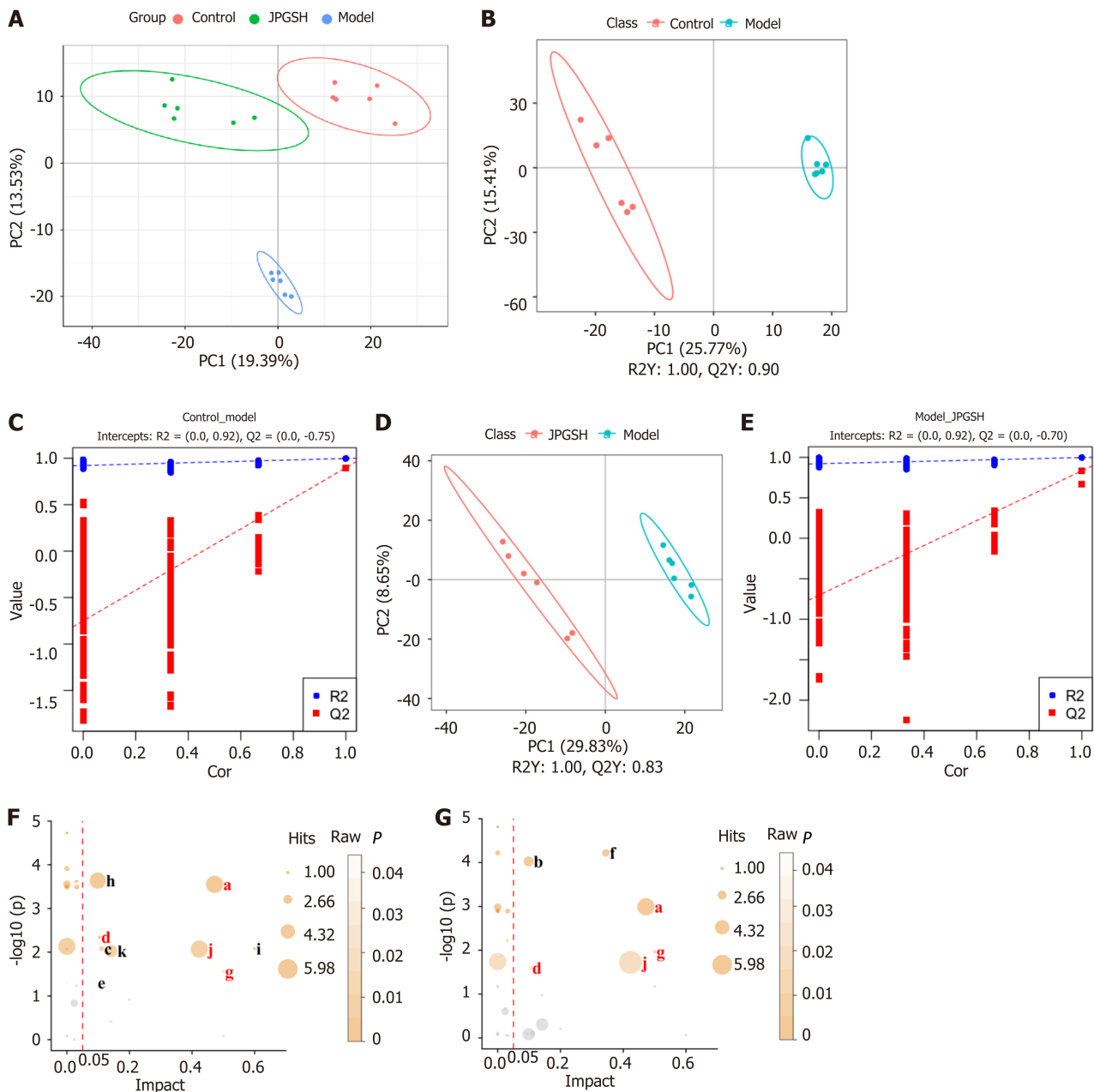


Figure 4 Jianpi Gushen Huayu Decoction treatment alters the metabolites in kidneys. A: Score plots of PCA among control, model, and high-dose Jianpi Gushen Huayu Decoction (JPGSH) groups; B and C: Score plots and permutation tests of partial least squares discriminant analysis (PLS-DA) between the control and model groups; D and E: Score plots and permutation tests of PLS-DA between the model and JPGSH groups; F: Results of the pathway analysis between the control and model groups; G: Results of the pathway analysis between the model and JPGSH groups. Common pathways are marked in red. The names of the pathways are represented by "a" to "k": a: Alanine, aspartate and glutamate metabolism; b: Arachidonic acid metabolism; c: Butanoate metabolism; d: Cysteine and methionine metabolism; e: Glycerophospholipid metabolism; f: Histidine metabolism; g: Riboflavin metabolism; h: Steroid hormone biosynthesis; i: Synthesis and degradation of ketone bodies; j: Tryptophan metabolism; k: Tyrosine metabolism. $n = 6$ per group. JPGSH: High-dose Jianpi Gushen Huayu Decoction.

by conducting metabolomics analyses. The results revealed that alanine, aspartate, and glutamate metabolism; cysteine and methionine metabolism; riboflavin metabolism; and tryptophan metabolism were the common metabolic pathways, signaling that the above pathways potentially functioned for treating DN.

The findings thus revealed that JPGS could regulate glucose metabolism and alanine, aspartate, and glutamate levels, which may be the underlying mechanism of ameliorating DN. Alanine, aspartate, and glutamate which are non-essential amino acids in humans, play a pivotal role in glycolysis and the tricarboxylic acid cycle; furthermore, their metabolism correlates closely with the progression of DM[35,36]. A study has suggested that alanine, aspartate, and glutamate levels in the sera of patients with DM as complicated by obesity were elevated and that glucose metabolism disorders induced by alanine, aspartate, and glutamate metabolism disorders potentially facilitated the progression of DM[37]. Alanine, a non-essential amino acid synthesized from pyruvate and branched chain amino acids, can increase glucose-dependent insulin secretion by inducing membrane depolarization during its co-transport with sodium ions[38]. Glutamate, synthesized from α -ketoglutaric acid produced by the deamination of glutamate under the action of glutaminase, can be oxidized to produce energy for the citric acid cycle independently of glucose[39] and to produce adenosine triphosphate

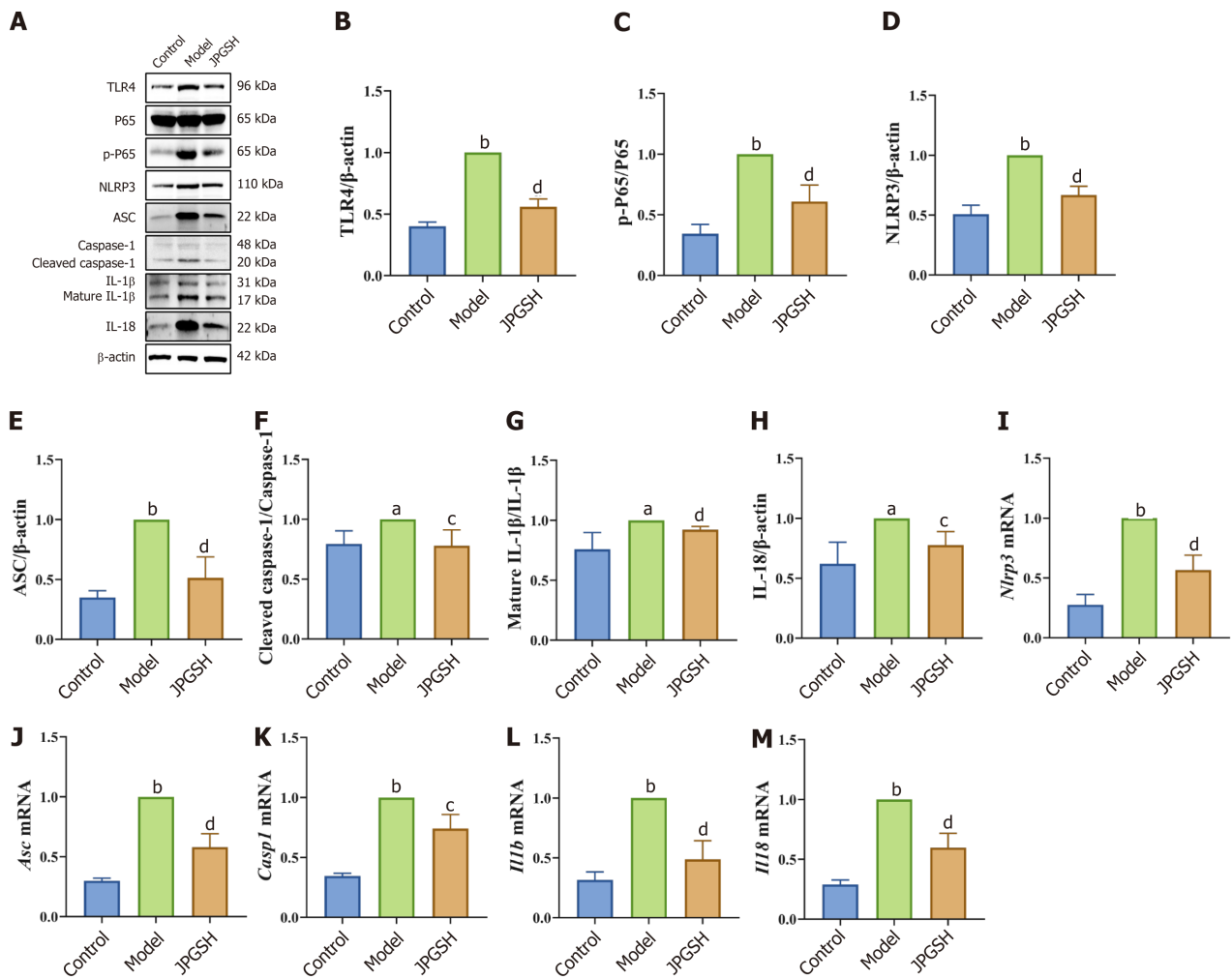


Figure 5 Jianpi Gushen Huayu Decoction moderated the toll-like receptor 4/nuclear factor-kappa B/NOD-like receptor family pyrin domain containing 3 pathway and ameliorated inflammatory injuries to kidneys. A: Western blotting results; B: Toll-like receptor 4 levels; C: p-P65/P65 levels; D: NOD-like receptor family pyrin domain containing 3 (NLRP3) levels; E: Apoptosis-associated speck-like protein containing a CARD (ASC) levels; F: Cleaved caspase-1/caspase-1 levels; G: Mature interleukin (IL)-1β/IL-1β levels; H: IL-18 levels; I: *Nlrp3* levels; J: *Asc* levels; K: *Casp1* levels; L: *Il1b* levels; M: *Il18* levels. ^a*P* < 0.05 as compared to the control group; ^b*P* < 0.01 as compared to the control group; ^c*P* < 0.05 as compared to the model group; ^d*P* < 0.01 as compared to the model group. J PGS: High-dose Jianpi Gushen Huayu Decoction; TLR4: toll-like receptor 4; NLRP3: NOD-like receptor family pyrin domain containing 3; ASC: Protein apoptosis-associated speck-like protein containing a CARD; IL: Interleukin.

to stimulate insulin secretion[38]. Additionally, a high level of glutamate can induce pancreatic β cell apoptosis, worsening DM[40]. Aspartate, produced by the hydrolysis of asparagine by L-asparaginase, participates in glucose production and maintaining a low level of aspartate in the blood can help reduce glycogen synthesis to diminish the risk of hyperlipidemia[41,42]. The above results indicate that glucose metabolism disorders could facilitate the progression of DM. The correlation between DN and alanine, aspartate, and glutamate metabolism remains scarcely investigated to date, and determining the underlying mechanism of J PGS requires further study.

In this study, J PGS could up-regulate the methionine level to regulate the methionine cycle and balance the *in vivo* homocysteine (Hcy) level to lessen kidney injury in DN mice. Cysteine and methionine are sulfur-containing amino acids. Cysteine is formed from serine and the condensation product of methionine-derived Hcy is used as the sulfur source. Methionine is an essential amino acid which animals cannot synthesize. Hcy, an intermediate metabolite of cysteine and methionine, plays a vital role in the progression of DN[43]. Hcy is a sulfur-containing non-essential amino acid and healthy kidneys are essential in Hcy clearance and metabolism; since the Hcy-specific tubular uptake mechanism and the metabolic enzymes of Hcy are present in the kidneys[44]. Studies showed that Hcy is a factor that affects urinary protein excretion independently of hypertension, DM, protein intake, and kidney function[45]. DN may be complicated by hyperhomocysteinemia (HHcy), whose pathogenesis is principally associated with the *in vivo* accumulation of Hcy caused by impaired glomerular filtration and Hcy metabolism disorder caused by the impaired integrity of the kidney structure and function. In addition, HHcy may exacerbate insulin resistance to contribute to the occurrence and progression of DN and HHcy and DN have a mutually exacerbating effect on each other[46]. The potential mechanism of treating DN by regulating cysteine and methionine metabolism must be studied further.

Our results indicated that J PGS could markedly up-regulate the riboflavin level in the kidney tissues of DN mice. Riboflavin, an essential nutrient for humans and animals, is a major food additive. Riboflavin performs critical metabolic functions by mediating electron transfer in biological redox reactions and participates in the metabolism of folate, vitamin

Table 1 Differential metabolites in kidney after Jianpi Gushen Huayu Decoction treatment

No.	Metabolites	Formula	RT (min)	m/z	FC		VIP		Trend		Pathway
					M vs C	J vs M	M vs C	J vs M	M vs C	J vs M	
1	15(S)-HpETE	C20H32O4	12.78	335.22	1.14	0.45	0.35	1.71	↑	↓ ^d	Arachidonic acid metabolism
2	16(R)-HETE	C20H32O3	13.91	343.22	1.23	0.28	0.58	1.69	↑	↓ ^d	Arachidonic acid metabolism
3	1-naphthol	C10H8O	8.86	145.06	3.00	0.53	1.51	1.19	↑ ^b	↓ ^c	
4	2-isopropylmalate	C7H12O5	1.32	175.06	1.97	2.06	1.61	1.37	↑ ^b	↑ ^c	
5	2-methoxyresorcinol	C7H8O3	11.65	141.05	1.21	1.20	1.37	1.34	↑ ^a	↑ ^c	
6	3-hydroxy-3-methyl-glutaric acid	C6H10O5	1.32	161.05	1.68	1.72	1.42	1.33	↑ ^a	↑ ^c	
7	3-indoleacrylic acid	C11H9NO2	6.03	186.06	0.52	1.63	1.83	1.38	↓ ^b	↑ ^c	
8	4-guanidinobutyric acid	C5H11N3O2	1.35	129.07	0.42	1.67	1.53	1.38	↓ ^b	↑ ^c	Butanoate metabolism
9	4-hydroxybenzoic acid	C7H6O3	5.73	137.02	0.57	3.72	1.39	1.65	↓ ^a	↑ ^d	
10	4-oxoretinol	C20H28O2	13.68	299.20	0.47	1.67	1.42	1.37	↓ ^a	↑ ^c	
11	5-hydroxyindole-3-acetic acid	C10H9NO3	7.05	192.07	7.50	0.04	1.31	1.44	↑ ^b	↓ ^d	Tryptophan metabolism
12	5-hydroxytryptophan	C11H12N2O3	6.55	221.09	0.23	2.30	1.50	1.65	↓ ^b	↑ ^d	Tryptophan metabolism
13	ACar 20:1	C27H52NO4	13.89	472.40	1.86	0.49	1.67	1.63	↑ ^b	↓ ^d	
14	Acetoacetate	C4H6O3	1.44	101.02	2.12	1.55	1.35	1.14	↑ ^a	↑	Arachidonic acid metabolism, synthesis and degradation of ketone bodies, tyrosine metabolism
15	Adrenosterone	C19H24O3	13.34	301.18	1.18	0.67	0.62	1.19	↑	↓ ^c	Steroid hormone biosynthesis
16	Alpha-ketoglutaric acid	C5H6O5	1.25	145.01	0.66	2.60	1.69	1.49	↓ ^b	↑ ^d	Alanine, aspartate and glutamate metabolism, butanoate metabolism
17	Anthranilic acid	C7H7NO2	1.55	138.06	0.71	3.98	1.26	1.83	↓ ^a	↑ ^d	Tryptophan metabolism
18	Asparagine	C4H8N2O3	1.24	131.05	0.41	5.12	1.33	0.91	↓ ^b	↑ ^c	Alanine, aspartate and glutamate metabolism
19	Biotin	C10H16N2O3S	8.15	245.10	0.94	2.00	0.21	1.51	↓	↑ ^d	
20	Cholesterol	C27H46O	15.23	387.36	0.84	1.51	0.78	1.29	↓	↑ ^c	Steroid hormone biosynthesis
21	Citraconic acid	C5H6O4	1.33	129.02	1.36	1.74	1.47	1.57	↑ ^a	↑ ^d	
22	Citric acid	C6H8O7	6.00	191.02	0.94	1.58	0.19	1.67	↓	↑ ^d	Alanine, aspartate and glutamate metabolism
23	Cnidioside A	C17H20O9	1.55	391.10	2.24	3.36	1.32	1.66	↑ ^a	↑ ^d	
24	Corey lactone diol	C8H12O4	1.30	171.07	1.31	1.91	1.23	1.61	↑ ^a	↑ ^d	
25	Cortisone	C21H28O5	11.25	361.20	1.85	0.56	1.46	1.44	↑ ^a	↓ ^c	Steroid hormone biosynthesis
26	D-glucosamine 6-phosphate	C6H14NO8P	1.20	258.04	1.02	0.58	0.10	1.37	↑	↓ ^c	Alanine, aspartate and glutamate metabolism
27	D-proline	C5H9NO2	1.54	116.07	0.60	1.97	1.64	1.63	↓ ^b	↑ ^d	
28	D-threose	C4H8O4	1.31	101.02	1.70	1.76	1.72	1.53	↑ ^b	↑ ^d	
29	Ecgonine	C9H15NO3	9.72	186.11	3.96	0.51	1.73	1.37	↑ ^b	↓ ^c	
30	Epitestosterone	C19H28O2	13.23	289.22	1.46	0.32	0.68	1.26	↑	↓ ^c	Steroid hormone biosynthesis
31	Estradiol	C18H24O2	14.93	273.18	0.92	0.62	0.34	1.17	↓	↓ ^c	Steroid hormone biosynthesis
32	Gamma-tocopherol	C28H48O2	13.26	417.37	2.17	0.36	1.38	1.44	↑ ^a	↓ ^d	
33	Glutaric acid	C5H8O4	1.43	131.03	1.49	1.93	1.26	1.60	↑ ^a	↑ ^d	
34	Guanidineacetic acid	C3H7N3O2	1.31	118.06	0.47	1.17	1.71	0.85	↓ ^b	↑	
35	Homovanillic acid	C9H10O4	2.09	181.05	0.52	1.40	1.90	1.20	↓ ^b	↑	Tyrosine metabolism

36	L-aspartic acid	C4H7NO4	1.21	132.03	1.67	0.35	0.50	1.46	↑ ^a	↓ ^d	Alanine, aspartate and glutamate metabolism
37	L-glutamine	C5H10N2O3	1.32	147.08	1.39	0.69	1.47	0.31	↑ ^a	↓ ^d	Alanine, aspartate and glutamate metabolism
38	L-histidine	C6H9N3O2	1.65	154.06	0.60	1.06	1.47	0.30	↓ ^a	↑	Histidine metabolism
39	L-kynurenine	C10H12N2O3	8.39	209.09	0.17	3.30	1.60	1.06	↓ ^b	↑ ^a	Tryptophan metabolism
40	L-thyroxine	C15H11I4NO4	11.98	775.68	0.59	0.79	1.36	0.72	↓ ^a	↓	Tyrosine metabolism
41	L-tryptophan	C11H12N2O2	6.70	205.10	0.25	3.24	1.55	1.06	↓ ^b	↑ ^d	Tryptophan metabolism
42	L-tyrosine	C9H11NO3	1.98	180.07	0.44	1.03	1.95	0.36	↓ ^b	↑	Tyrosine metabolism
43	Metanephrine	C10H15NO3	8.92	196.10	3.35	0.21	1.25	1.30	↑ ^a	↓ ^c	Tyrosine metabolism
44	Methionine	C5H11NO2S	1.43	150.06	0.17	3.10	1.67	1.62	↓ ^b	↑ ^d	Cysteine and methionine metabolism
45	N-acetylaspartic acid	C6H9NO5	1.21	128.04	1.00	0.54	0.07	1.53	↑	↓ ^d	Alanine, aspartate and glutamate metabolism
46	N-acetylserotonin	C12H14N2O2	7.25	219.11	0.29	2.46	1.23	1.44	↓ ^a	↑ ^d	Tryptophan metabolism
47	Oxoadipic acid	C6H8O5	1.20	159.03	0.54	2.37	1.35	1.52	↓ ^b	↑ ^d	Tryptophan metabolism
48	PC (16:0/16:0)	C40H80NO8P	16.96	734.57	0.67	1.64	1.18	1.85	↓	↑ ^d	Arachidonic acid metabolism, glycerophospholipid metabolism
49	Prostaglandin D2	C20H32O5	11.09	351.22	0.87	0.46	0.36	1.26	↓	↓ ^c	Arachidonic acid metabolism
50	Urocanic acid	C6H6N2O2	1.76	139.05	1.61	1.05	1.23	0.54	↑ ^a	↑	Histidine metabolism
51	Vitamin B2	C17H20N4O6	7.92	377.15	0.17	4.09	1.48	1.69	↓ ^b	↑ ^d	Riboflavin metabolism

^a*P* < 0.05 as compared to the control group.

^b*P* < 0.01 as compared to the control group.

^c*P* < 0.05 as compared to the model group.

^d*P* < 0.01 as compared to the model group.

C: Control group; M: Model group; J: High-dose Jianpi Gushen Huayu Decoction group, *n* = 6 per group; RT: Retention time; VIP: Variable importance for the projection; FC: Fold change.

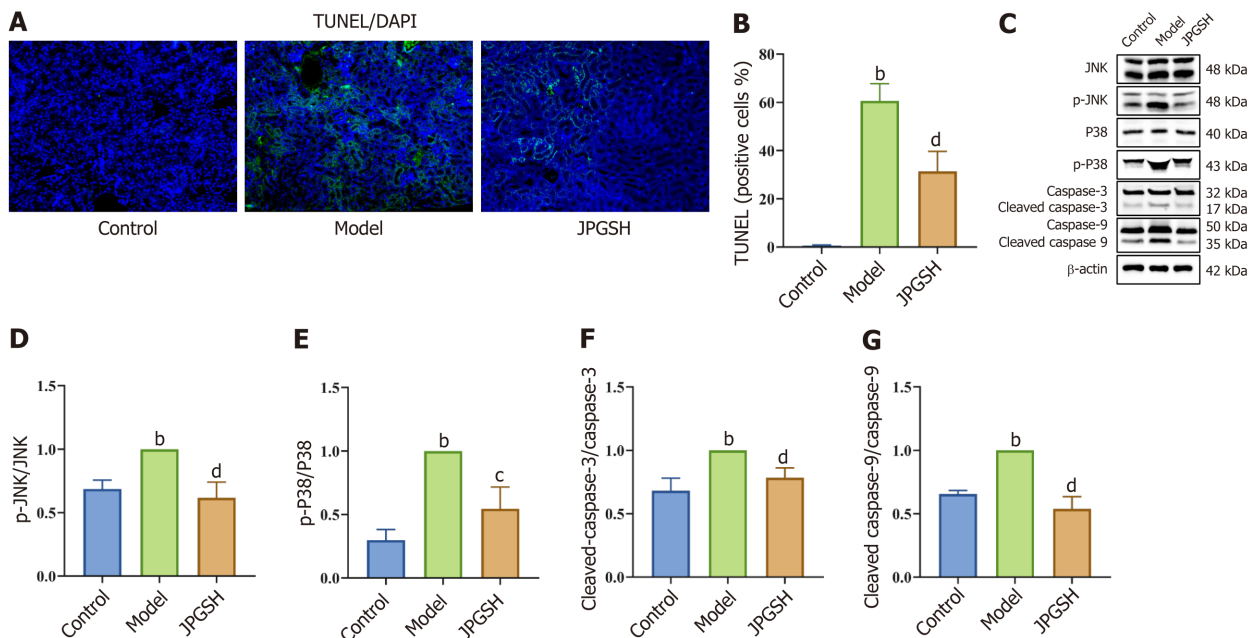


Figure 6 Jianpi Gushen Huayu Decoction inhibited c-Jun N-terminal kinase/P38 pathway mediated apoptosis and improved kidney injury.

A: TUNEL staining; B: Percentage of positive cells in TUNEL staining; C: Western blotting results; D: p-c-Jun N-terminal kinase (JNK)/JNK level; E: p-P38/P38 levels; F: Cleaved-caspase-3/caspase-3 levels; G: Cleaved caspase-9/caspase-9 levels. ^b*P* < 0.01 as compared to the control group; ^c*P* < 0.05 as compared to the model group; ^d*P* < 0.01 as compared to the model group. JPGSH: High-dose Jianpi Gushen Huayu Decoction; JNK: c-Jun N-terminal kinase.

B12, vitamin B6, and other vitamins[47]. Riboflavin, a precursor for flavin mononucleotide and flavin adenine dinucleotide (FAD), serves as a coenzyme for multiple oxidases and dehydrogenases in eucaryotic cells[48]. FAD-dependent Ero1 and sulfhydryl oxidases are involved in secretory proteins oxidative folding, leading to the formation of disulfide bonds[49-52]. Riboflavin deficiency could lead to impaired oxidative folding, resulting in various clinical abnormalities (e.g., kidney injury)[49,50,53]. A study suggested that riboflavin notably inhibited the production of lipid peroxides, enhanced the SOD level, effectively inhibited the connective tissue growth factor (that could significantly exacerbate fibrosis) and showed desirable antioxidant effects in DM rats injected with STZ. This signaled that riboflavin potentially protects against DM-associated systemic fibrosis[54]. Therefore, the effects of JPGS on inhibiting oxidative stress and improving fibrosis in DN mice were possibly related to the regulation of riboflavin metabolism. In future studies, the relationships between the effect of JPGS on regulating riboflavin metabolism and its antioxidant and anti-fibrosis effects should be illuminated.

Furthermore, our findings revealed that tryptophan metabolism disorder occurred in the kidneys of DN model mice; in addition, 5-hydroxytryptophan (5-HTP) and NAS contents decreased to varying degrees, whereas 5-HIAA content increased noticeably. JPGS could restore the levels of the above metabolites. This indicated that JPGS could significantly regulate tryptophan metabolism. Tryptophan, one of the eight essential amino acids in humans, plays a fundamental role in human health and diseases[55]. Tryptophan is principally metabolized *via* 5-hydroxytryptamine (5-HT), kynurenine (KYN), and indole pathways[55]. In the 5-HT pathway, tryptophan is hydroxylated by tryptophan hydroxylase to yield 5-HTP, which is catalyzed by 5-HTP decarboxylase to yield 5-HT. Then, 5-HT reacts with acetyl coenzyme A, as catalyzed by N-acetyltransferase, to form NAS. Recent studies showed that 5-HTP, an effective anti-inflammatory mediator, inhibited the activation of P38 and NF- κ B in fibroblasts, reduced the expression levels of inflammatory factors in peripheral blood mononuclear cells[56,57], and inhibited the production of TNF- α induced by lipopolysaccharides to improve inflammatory responses[58,59]. Therefore, JPGS may reduce the TNF- α level by up-regulating the 5-HTP level. A study has reported that 5-HTP could reduce mammary epithelial cell apoptosis in goats *via* the MAPK/extracellular signal-regulated kinase/B-cell lymphoma-3 pathway[60]. NAS, a melatonin precursor, offers anti-inflammatory and antioxidant effects[61]. Another study has suggested that melatonin could mitigate white matter injury in rats subjected to focal ischemia-reperfusion injuries by inhibiting the activation of TLR4/NF- κ B pathways, indicating that NAS may regulate the TLR4/NF- κ B pathway[62]. Liu *et al*[19] investigated retinal ischemia-reperfusion injury (RIRI) and found that NAS could reduce retinal injuries in rats subjected to RIRI through blocking the activation of the TLR4/NF- κ B/NLRP3 pathway to inhibit the expression of IL-1 β . 5-HIAA, a metabolic end product of 5-HTP, has been proven to promote apoptosis and activate JNK/P38 pathway-mediated apoptosis[20]. Moreover, tryptophan is the only source of the KYN pathway. In the KYN approach, tryptophan is catabolized into KYN as regulated by indoleamine 2,3-dioxygenase and tryptophan-2,3-dioxygenase, and then KYN is metabolized into downstream metabolites (e.g., kynuric, xanthic, and quinolinic acids), which participate in immune activation and inflammation regulation and are associated with obesity and insulin resistance[55,63,64].

Considering the effect of tryptophan metabolism on significantly modulating the TLR4/NF- κ B/NLRP3 pathway, we investigated the effect of JPGS on the TLR4/NF- κ B/NLRP3 pathway in DN model mice. The study results exhibited that JPGS could restrain the activation of the TLR4/NF- κ B/NLRP3 pathway in kidneys. TLR4, a member of the TLR family, plays a crucial role in the cellular antioxidant response and the production of inflammatory cytokines and its activation can lead to NF- κ B activation[65-67]. Normally, the NF- κ B dimer in the cytoplasm binds to I κ B α to form a complex. When I κ B α phosphorylation is inactivated, NF- κ B is activated and translocated to the nucleus to activate glial cells in order to secrete numerous pro-inflammatory molecules (e.g., IL-1 β , IL-18, TNF- α , and IL-6) and induce the expression of the NLRP3 inflammasome[68,69]. The NLRP3 inflammasome is a multi-protein complex composed of NLRP3, ASC, and caspase-1. Activating NLRP3 can promote the assembly of various components (NLRP3, ASC, and caspase-1) of NLRP3 inflammasome to activate pro-caspase-1 to produce active cleaved caspase-1 which, in turn, cleaves and matures the inflammatory factors IL-1 β and IL-18. Mature IL-1 β can further stimulate the secretion of large quantities of pro-IL-1 β , creating a positive feedback loop that amplifies immune responses by activating the NF- κ B. As such, DN-related kidney injury can be effectively improved by reducing the activation of the TLR4/NF- κ B/NLRP3 pathway[70].

Considering the effects of tryptophan metabolites in markedly regulating JNK/P38-mediated apoptosis, we investigated the effect of JPGS on JNK/P38-mediated apoptosis in DN mice. The study results revealed that JPGS could restrain the activation of the JNK/P38 to reduce kidney cell apoptosis in DN mice. TUNEL staining is commonly employed to assess cell apoptosis in body tissues. In this study, it has been determined that JPGS can effectively reduce apoptosis in the kidney tissues of DN mice. JNK and P38-MAPK family members play a central role in inducing cell apoptosis. JNK, a type of serine-threonine kinase, can be activated by multiple factors (e.g., stress and inflammatory cytokines). Activated JNK is translocated from the cytoplasm to the nucleus to further induce the mRNA transcription of pro-apoptotic factors (e.g., p53, Fas ligand, TNF, and Bax) and to act on mitochondria. For example, Bax and Bak promote the production of cytochrome C in cytoplasm so that cytochrome C binds to caspase-9 to act on caspase-3. Activated caspase-3 binds to apoptotic substrates to cause cell apoptosis[71]. JNK and P38 are stress-activated protein kinases and some factors can activate both JNK and P38 pathways. Activated P38 can induce cell apoptosis by increasing c-myc expression, phosphorylating P53, inducing Bax translocation, and enhancing TNF- α expression[71]. As oxidative stress occurs and increased levels of inflammatory factors are present in DN patients, the JNK/P38 signaling pathway is activated to exacerbate kidney cell apoptosis[72]. As such, kidney injury in DN patients can be improved by inhibiting JNK/P38-mediated apoptosis[73].

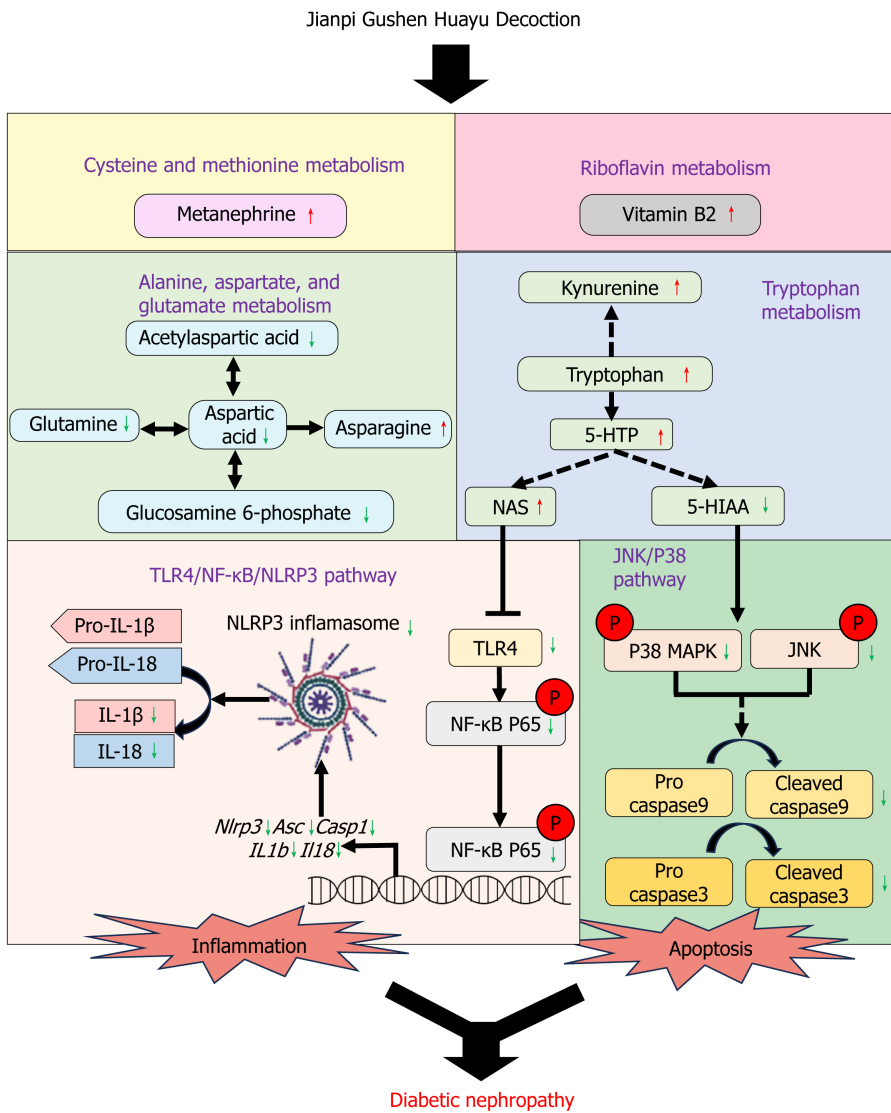


Figure 7 Jianpi Gushen Huayu Decoction could improve kidney inflammatory responses and kidney injury in diabetic nephropathy mice via the toll-like receptor 4/nuclear factor-kappa B/NOD-like receptor family pyrin domain containing 3 pathway and inhibit kidney cell apoptosis in diabetic nephropathy mice via the JNK/P38 pathway. It is possibly related to regulate cysteine and methionine metabolism, alanine, aspartate, and glutamate metabolism, tryptophan metabolism and riboflavin metabolism in kidney. NF-κB: Nuclear factor-kappa B; 5-HHTP: 5-hydroxytryptophan; NAS: N-acetylserotonin; 5-HIAA: 5-hydroxyindole-3-acetic acid; JNK: c-Jun N-terminal kinase; TLR4: toll-like receptor 4; NLRP3: NOD-like receptor family pyrin domain containing 3; ASC: Protein apoptosis-associated speck-like protein containing a CARD; IL: Interleukin.

CONCLUSION

Our results revealed that JPGS could markedly treat mice with STZ-induced DN. The metabolomics results exhibited that the efficacy of JPGS is possibly related to cysteine and methionine metabolism; alanine, aspartate, and glutamate metabolism; tryptophan metabolism; and riboflavin metabolism. Furthermore, JPGS could improve kidney inflammatory responses and kidney injury in DN mice via the TLR4/NF-κB/NLRP3 pathway and may inhibit kidney cell apoptosis in DN mice via the JNK/P38 pathway (Figure 7).

ARTICLE HIGHLIGHTS

Research background

As a frequent complication of type 2 diabetes mellitus, diabetic nephropathy (DN) is insidious and highly prevalent. The dysfunction of metabolism is closely related to the progression of diabetes and diabetic complications. Regulating metabolism to ameliorate DN has recently become a well explored research area.

Research motivation

Jianpi Gushen Huayu Decoction (JPGS) is highly efficacious clinically on DN, nevertheless, its renoprotective mechanism of action on DN has not yet been intensively investigated.

Research objectives

To evaluate the therapeutic effects and the possible mechanism of JPGS on DN based on untargeted metabolomics.

Research methods

The therapeutic potentials of JPGS was first evaluated on a DN mouse model. Then, the effect of JPGS on the kidney metabolite levels in DN mice was tested using non-targeted metabolomics. Furthermore, the effects of JPGS on c-Jun N-terminal kinase (JNK)/P38-mediated apoptosis and inflammatory responses mediated by toll-like receptor 4 (TLR4)/nuclear factor-kappaB (NF-κB)/NOD-like receptor family pyrin domain containing 3 (NLRP3) were examined.

Research results

JPGS administration improved body weight loss, hyperglycemia, kidney injury, and factors of oxidative stress and inflammation in DN mice. In addition, JPGS altered 51 differential metabolites of kidney in DN mice. Pathways related to cysteine and methionine metabolism, alanine, tryptophan metabolism, aspartate and glutamate metabolism, and riboflavin metabolism were identified as the key pathway of JPGS on DN. Further experimental validation showed that JPGS treatment reduced the expression of expression of TLR4/NF-κB/NLRP3 pathway and JNK/P38 pathway-mediated apoptosis related factors.

Research conclusions

JPGS could improve kidney inflammatory responses and kidney injury in DN mice *via* the TLR4/NF-κB/NLRP3 pathway and inhibit kidney cell apoptosis in DN mice *via* the JNK/P38 pathway. It is possibly related to regulate cysteine and methionine metabolism, alanine, aspartate, and glutamate metabolism, tryptophan metabolism and riboflavin metabolism in kidney.

Research perspectives

This study can provide scientific evidence for the clinical use of JPGS. Moreover, our study can be a useful for researchers in studying the relationship between metabolites and pathways in drug intervention.

FOOTNOTES

Author contributions: Cui HT and Lv SQ conceived and designed the study; Ma ZA, Wang LX, Zhang H, and Li HZ conducted the experiments and obtained the data; Li HZ, Dong L, and Wang QH analyzed and collated the data; Ma ZA, Wang YS, and Pan BC drafted and written the final version of the manuscript; Zhang SF, Cui HT, and Lv SQ contributed equally to this work; and all authors approved the final version of the manuscript.

Supported by the Scientific Foundation of Administration of Traditional Chinese Medicine of Hebei Province, China, No. 2023257.

Institutional animal care and use committee statement: The animal study was reviewed and approved by Ethics Committee of Hebei University of Chinese Medicine (Approval No. CZX2021-KY-026).

Conflict-of-interest statement: All the authors report no relevant conflicts of interest for this article.

Data sharing statement: The original contributions presented in the study are included in the article/supplementary material. Further inquiries can be directed to the corresponding authors.

ARRIVE guidelines statement: The authors have read the ARRIVE guidelines, and the manuscript was prepared and revised according to the ARRIVE guidelines.

Open-Access: This article is an open-access article that was selected by an in-house editor and fully peer-reviewed by external reviewers. It is distributed in accordance with the Creative Commons Attribution NonCommercial (CC BY-NC 4.0) license, which permits others to distribute, remix, adapt, build upon this work non-commercially, and license their derivative works on different terms, provided the original work is properly cited and the use is non-commercial. See: <https://creativecommons.org/licenses/by-nc/4.0/>

Country/Territory of origin: China

ORCID number: Huan-Tian Cui 0000-0002-0820-5436; Shu-Quan Lv 0000-0002-7129-3934.

S-Editor: Wang JJ

L-Editor: A

P-Editor: Zhang YL

REFERENCES

- 1 Selby NM, Taal MW. An updated overview of diabetic nephropathy: Diagnosis, prognosis, treatment goals and latest guidelines. *Diabetes Obes Metab* 2020; **22** Suppl 1: 3-15 [PMID: 32267079 DOI: 10.1111/dom.14007]
- 2 Rodriguez F, Lee DJ, Gad SS, Santos MP, Beetel RJ, Vasey J, Bailey RA, Patel A, Blais J, Weir MR, Dash R. Real-World Diagnosis and Treatment of Diabetic Kidney Disease. *Adv Ther* 2021; **38**: 4425-4441 [PMID: 34254257 DOI: 10.1007/s12325-021-01777-9]
- 3 Hu Q, Chen Y, Deng X, Li Y, Ma X, Zeng J, Zhao Y. Diabetic nephropathy: Focusing on pathological signals, clinical treatment, and dietary regulation. *Biomed Pharmacother* 2023; **159**: 114252 [PMID: 36641921 DOI: 10.1016/j.biopha.2023.114252]
- 4 Nie Q, Chen H, Hu J, Fan S, Nie S. Dietary compounds and traditional Chinese medicine ameliorate type 2 diabetes by modulating gut microbiota. *Crit Rev Food Sci Nutr* 2019; **59**: 848-863 [PMID: 30569745 DOI: 10.1080/10408398.2018.1536646]
- 5 Zu G, Sun K, Li L, Zu X, Han T, Huang H. Mechanism of quercetin therapeutic targets for Alzheimer disease and type 2 diabetes mellitus. *Sci Rep* 2021; **11**: 22959 [PMID: 34824300 DOI: 10.1038/s41598-021-02248-5]
- 6 Samaha MM, Said E, Salem HA. A comparative study of the role of crocin and sitagliptin in attenuation of STZ-induced diabetes mellitus and the associated inflammatory and apoptotic changes in pancreatic β -islets. *Environ Toxicol Pharmacol* 2019; **72**: 103238 [PMID: 31394428 DOI: 10.1016/j.etap.2019.103238]
- 7 Yin B, Bi YM, Fan GJ, Xia YQ. Molecular Mechanism of the Effect of Huanglian Jiedu Decoction on Type 2 Diabetes Mellitus Based on Network Pharmacology and Molecular Docking. *J Diabetes Res* 2020; **2020**: 5273914 [PMID: 33134394 DOI: 10.1155/2020/5273914]
- 8 Muthubharathi BC, Gowriprya T, Balamurugan K. Metabolomics: small molecules that matter more. *Mol Omics* 2021; **17**: 210-229 [PMID: 33598670 DOI: 10.1039/d0mo00176g]
- 9 Du Y, Xu BJ, Deng X, Wu XW, Li YJ, Wang SR, Wang YN, Ji S, Guo MZ, Yang DZ, Tang DQ. Predictive metabolic signatures for the occurrence and development of diabetic nephropathy and the intervention of Ginkgo biloba leaves extract based on gas or liquid chromatography with mass spectrometry. *J Pharm Biomed Anal* 2019; **166**: 30-39 [PMID: 30599279 DOI: 10.1016/j.jpba.2018.12.017]
- 10 Yaribeygi H, Zare V, Butler AE, Barreto GE, Sahebkar A. Antidiabetic potential of saffron and its active constituents. *J Cell Physiol* 2019; **234**: 8610-8617 [PMID: 30515777 DOI: 10.1002/jcp.27843]
- 11 Chen L, Lu X, El-Seedi H, Teng H. Recent advances in the development of sesquiterpenoids in the treatment of type 2 diabetes. *Trends Food Sci Tech* 2019; **88**: 46-56 [DOI: 10.1016/j.tifs.2019.02.003]
- 12 Zhou Y, Zhang MX, Zhang YN, Liu ZQ, Song FR, Zhao CF. Fecal metabolomics study of radix scutellariae's effect on treating type 2 diabetic rats based on mass spectrometry technique. *J Chinese Mass Spectrometry Society* 2018; **39**: 679-686 [DOI: 10.7538/zpxb.2018.0034]
- 13 Dai X, Su S, Cai H, Wei D, Yan H, Zheng T, Zhu Z, Shang EX, Guo S, Qian D, Duan JA. Protective Effects of Total Glycoside From Rehmannia glutinosa Leaves on Diabetic Nephropathy Rats via Regulating the Metabolic Profiling and Modulating the TGF- β 1 and Wnt/ β -Catenin Signaling Pathway. *Front Pharmacol* 2018; **9**: 1012 [PMID: 30271343 DOI: 10.3389/fphar.2018.01012]
- 14 Qin Z, Wang W, Liao W, Wu X, Li X. UPLC-Q/TOF-MS-Based Serum Metabolomics Reveals Hypoglycemic Effects of Rehmannia glutinosa, Coptis chinensis and Their Combination on High-Fat-Diet-Induced Diabetes in KK-Ay Mice. *Int J Mol Sci* 2018; **19** [PMID: 30544908 DOI: 10.3390/ijms19123984]
- 15 Wang Z, Fu W, Huo M, He B, Liu Y, Tian L, Li W, Zhou Z, Wang B, Xia J, Chen Y, Wei J, Abliz Z. Spatial-resolved metabolomics reveals tissue-specific metabolic reprogramming in diabetic nephropathy by using mass spectrometry imaging. *Acta Pharm Sin B* 2021; **11**: 3665-3677 [PMID: 34900545 DOI: 10.1016/j.apsb.2021.05.013]
- 16 Jia CX, Lv SQ. [Observation on the therapeutic effect of jianpi gushen huayu decoction on diabetic nephropathy of type of spleen - kidney deficiency with stasis at clinical period]. *Modern J Integrated Tradit Chi Western Med* 2020; **29**: 1851-1855
- 17 Alzahrani FA. Melatonin improves therapeutic potential of mesenchymal stem cells-derived exosomes against renal ischemia-reperfusion injury in rats. *Am J Transl Res* 2019; **11**: 2887-2907 [PMID: 31217862]
- 18 Yang YY, Shi LX, Li JH, Yao LY, Xiang DX. Piperazine ferulate ameliorates the development of diabetic nephropathy by regulating endothelial nitric oxide synthase. *Mol Med Rep* 2019; **19**: 2245-2253 [PMID: 30664213 DOI: 10.3892/mmr.2019.9875]
- 19 Liu J, Zhang N, Zhang M, Yin H, Zhang X, Wang X, Zhao Y. N-acetylserotonin alleviated the expression of interleukin-1 β in retinal ischemia-reperfusion rats via the TLR4/NF- κ B/NLRP3 pathway. *Exp Eye Res* 2021; **208**: 108595 [PMID: 34000276 DOI: 10.1016/j.exer.2021.108595]
- 20 Jeong YM, Li H, Kim SY, Park WJ, Yun HY, Baek KJ, Kwon NS, Jeong JH, Myung SC, Kim DS. Photo-activated 5-hydroxyindole-3-acetic acid induces apoptosis of prostate and bladder cancer cells. *J Photochem Photobiol B* 2011; **103**: 50-56 [PMID: 21310627 DOI: 10.1016/j.jphotobiol.2011.01.011]
- 21 Huang W, Man Y, Gao C, Zhou L, Gu J, Xu H, Wan Q, Long Y, Chai L, Xu Y. Short-Chain Fatty Acids Ameliorate Diabetic Nephropathy via GPR43-Mediated Inhibition of Oxidative Stress and NF- κ B Signaling. *Oxid Med Cell Longev* 2020; **2020**: 4074832 [PMID: 32831998 DOI: 10.1155/2020/4074832]
- 22 Ju Y, Su Y, Chen Q, Ma K, Ji T, Wang Z, Li W. Protective effects of Astragaloside IV on endoplasmic reticulum stress-induced renal tubular epithelial cells apoptosis in type 2 diabetic nephropathy rats. *Biomed Pharmacother* 2019; **109**: 84-92 [PMID: 30396095 DOI: 10.1016/j.biopha.2018.10.041]
- 23 Huang Y, Liu W, Liu J, Guo D, Zhang P, Liu D, Lin J, Yang L, Zhang H, Xue Y. Association of Urinary Sodium Excretion and Diabetic Kidney Disease in Patients With Type 2 Diabetes Mellitus: A Cross-Sectional Study. *Front Endocrinol (Lausanne)* 2021; **12**: 772073 [PMID: 34777262 DOI: 10.3389/fendo.2021.772073]
- 24 Ronco C, Bellomo R, Kellum JA. Acute kidney injury. *Lancet* 2019; **394**: 1949-1964 [PMID: 31777389 DOI: 10.1016/S0140-6736(19)32563-2]
- 25 Levey AS, James MT. Acute Kidney Injury. *Ann Intern Med* 2017; **167**: ITC66-ITC80 [PMID: 29114754 DOI: 10.7326/AITC201711070]
- 26 Parving HH, Lehnert H, Bröchner-Mortensen J, Gomis R, Andersen S, Arner P; Irbesartan in Patients with Type 2 Diabetes and Microalbuminuria Study Group. The effect of irbesartan on the development of diabetic nephropathy in patients with type 2 diabetes. *N Engl J Med* 2001; **345**: 870-878 [PMID: 11565519 DOI: 10.1056/NEJMoa011489]
- 27 Hu R, Wang MQ, Ni SH, Wang M, Liu LY, You HY, Wu XH, Wang YJ, Lu L, Wei LB. Salidroside ameliorates endothelial inflammation and oxidative stress by regulating the AMPK/NF- κ B/NLRP3 signaling pathway in AGEs-induced HUVECs. *Eur J Pharmacol* 2020; **867**: 172797 [PMID: 31747547 DOI: 10.1016/j.ejphar.2019.172797]
- 28 Stieger N, Worthmann K, Teng B, Engeli S, Das AM, Haller H, Schiffer M. Impact of high glucose and transforming growth factor- β on bioenergetic profiles in podocytes. *Metabolism* 2012; **61**: 1073-1086 [PMID: 22365040 DOI: 10.1016/j.metabol.2011.12.003]

- 29 **Karunasagara S**, Hong GL, Park SR, Lee NH, Jung DY, Kim TW, Jung JY. Korean red ginseng attenuates hyperglycemia-induced renal inflammation and fibrosis via accelerated autophagy and protects against diabetic kidney disease. *J Ethnopharmacol* 2020; **254**: 112693 [PMID: 32112899 DOI: 10.1016/j.jep.2020.112693]
- 30 **Qiao S**, Liu R, Lv C, Miao Y, Yue M, Tao Y, Wei Z, Xia Y, Dai Y. Bergein impedes the generation of extracellular matrix in glomerular mesangial cells and ameliorates diabetic nephropathy in mice by inhibiting oxidative stress via the mTOR/ β -TrCP/Nrf2 pathway. *Free Radic Biol Med* 2019; **145**: 118-135 [PMID: 31494242 DOI: 10.1016/j.freeradbiomed.2019.09.003]
- 31 **Samsu N**. Diabetic Nephropathy: Challenges in Pathogenesis, Diagnosis, and Treatment. *Biomed Res Int* 2021; **2021**: 1497449 [PMID: 34307650 DOI: 10.1155/2021/1497449]
- 32 **Ma L**, Wu F, Shao Q, Chen G, Xu L, Lu F. Baicalin Alleviates Oxidative Stress and Inflammation in Diabetic Nephropathy via Nrf2 and MAPK Signaling Pathway. *Drug Des Devel Ther* 2021; **15**: 3207-3221 [PMID: 34321869 DOI: 10.2147/DDDT.S319260]
- 33 **Dinarello CA**. Proinflammatory cytokines. *Chest* 2000; **118**: 503-508 [PMID: 10936147 DOI: 10.1378/chest.118.2.503]
- 34 **Schrijvers BF**, De Vriese AS, Flyvbjerg A. From hyperglycemia to diabetic kidney disease: the role of metabolic, hemodynamic, intracellular factors and growth factors/cytokines. *Endocr Rev* 2004; **25**: 971-1010 [PMID: 15583025 DOI: 10.1210/er.2003-0018]
- 35 **Engskog MK**, Ersson L, Haglöf J, Arvidsson T, Pettersson C, Brittebo E. β -N-Methylamino-L-alanine (BMAA) perturbs alanine, aspartate and glutamate metabolism pathways in human neuroblastoma cells as determined by metabolic profiling. *Amino Acids* 2017; **49**: 905-919 [PMID: 28161796 DOI: 10.1007/s00726-017-2391-8]
- 36 **Roointan A**, Gheisari Y, Hudkins KL, Gholaminejad A. Non-invasive metabolic biomarkers for early diagnosis of diabetic nephropathy: Meta-analysis of profiling metabolomics studies. *Nutr Metab Cardiovasc Dis* 2021; **31**: 2253-2272 [PMID: 34059383 DOI: 10.1016/j.numecd.2021.04.021]
- 37 **Sookoian S**, Pirola CJ. Liver enzymes, metabolomics and genome-wide association studies: from systems biology to the personalized medicine. *World J Gastroenterol* 2015; **21**: 711-725 [PMID: 25624707 DOI: 10.3748/wjg.v21.i3.711]
- 38 **Herchuelz A**, Lebrun P, Boschero AC, Malaisse WJ. Mechanism of arginine-stimulated Ca^{2+} influx into pancreatic B cell. *Am J Physiol* 1984; **246**: E38-E43 [PMID: 6320660 DOI: 10.1152/ajpendo.1984.246.1.E38]
- 39 **Hosios AM**, Hecht VC, Danai LV, Johnson MO, Rathmell JC, Steinhilber ML, Manalis SR, Vander Heiden MG. Amino Acids Rather than Glucose Account for the Majority of Cell Mass in Proliferating Mammalian Cells. *Dev Cell* 2016; **36**: 540-549 [PMID: 26954548 DOI: 10.1016/j.devcel.2016.02.012]
- 40 **Banday VS**, Lejon K. Elevated systemic glutamic acid level in the non-obese diabetic mouse is Idd linked and induces beta cell apoptosis. *Immunology* 2017; **150**: 162-171 [PMID: 27649685 DOI: 10.1111/imm.12674]
- 41 **Aikawa T**, Matsutaka H, Takezawa K, Ishikawa E. Gluconeogenesis and amino acid metabolism. I. Comparison of various precursors for hepatic gluconeogenesis in vivo. *Biochim Biophys Acta* 1972; **279**: 234-244 [PMID: 5082497 DOI: 10.1016/0304-4165(72)90139-0]
- 42 **Chung ST**, Courville AB, Onuzuruie AU, Galvan-De La Cruz M, Mabundo LS, DuBose CW, Kasturi K, Cai H, Gharib AM, Walter PJ, Garraffo HM, Chacko S, Haymond MW, Sumner AE. Gluconeogenesis and risk for fasting hyperglycemia in Black and White women. *JCI Insight* 2018; **3** [PMID: 30232289 DOI: 10.1172/jci.insight.121495]
- 43 **Hofmann MA**, Kohl B, Zumbach MS, Borcea V, Bierhaus A, Henkels M, Amiral J, Schmidt AM, Fiehn W, Ziegler R, Wahl P, Nawroth PP. Hyperhomocyst(e)inemia and endothelial dysfunction in IDDM. *Diabetes Care* 1998; **21**: 841-848 [PMID: 9589252 DOI: 10.2337/diacare.21.5.841]
- 44 **Friedman AN**, Bostom AG, Selhub J, Levey AS, Rosenberg IH. The kidney and homocysteine metabolism. *J Am Soc Nephrol* 2001; **12**: 2181-2189 [PMID: 11562419 DOI: 10.1681/ASN.V12102181]
- 45 **Li Z**, Han Q, Ye H, Li J, Wei X, Zhang R, Huang Q, Xu Y, Liu G, Li B, Yang Q. Serum homocysteine is associated with tubular interstitial lesions at the early stage of IgA nephropathy. *BMC Nephrol* 2022; **23**: 78 [PMID: 35196994 DOI: 10.1186/s12882-021-02632-3]
- 46 **Muzurović E**, Kraljević I, Solak M, Dragnić S, Mikhailidis DP. Homocysteine and diabetes: Role in macrovascular and microvascular complications. *J Diabetes Complications* 2021; **35**: 107834 [PMID: 33419630 DOI: 10.1016/j.jdiacomp.2020.107834]
- 47 **Hustad S**, McKinley MC, McNulty H, Schneede J, Strain JJ, Scott JM, Ueland PM. Riboflavin, flavin mononucleotide, and flavin adenine dinucleotide in human plasma and erythrocytes at baseline and after low-dose riboflavin supplementation. *Clin Chem* 2002; **48**: 1571-1577 [PMID: 12194936]
- 48 **Suwannasom N**, Kao I, Pruß A, Georgieva R, Bäuml H. Riboflavin: The Health Benefits of a Forgotten Natural Vitamin. *Int J Mol Sci* 2020; **21** [PMID: 32023913 DOI: 10.3390/ijms21030950]
- 49 **Camporeale G**, Zempleni J. Oxidative folding of interleukin-2 is impaired in flavin-deficient jurkat cells, causing intracellular accumulation of interleukin-2 and increased expression of stress response genes. *J Nutr* 2003; **133**: 668-672 [PMID: 12612135 DOI: 10.1093/jn/133.3.668]
- 50 **Manthey KC**, Chew YC, Zempleni J. Riboflavin deficiency impairs oxidative folding and secretion of apolipoprotein B-100 in HepG2 cells, triggering stress response systems. *J Nutr* 2005; **135**: 978-982 [PMID: 15867268 DOI: 10.1093/jn/135.5.978]
- 51 **Thorpe C**, Hooper KL, Raje S, Glynn NM, Burnside J, Turi GK, Coppock DL. Sulfhydryl oxidases: emerging catalysts of protein disulfide bond formation in eukaryotes. *Arch Biochem Biophys* 2002; **405**: 1-12 [PMID: 12176051 DOI: 10.1016/S0003-9861(02)00337-5]
- 52 **Tu BP**, Ho-Schleyer SC, Travers KJ, Weissman JS. Biochemical basis of oxidative protein folding in the endoplasmic reticulum. *Science* 2000; **290**: 1571-1574 [PMID: 11090354 DOI: 10.1126/science.290.5496.1571]
- 53 **Alam MM**, Iqbal S, Naseem I. Ameliorative effect of riboflavin on hyperglycemia, oxidative stress and DNA damage in type-2 diabetic mice: Mechanistic and therapeutic strategies. *Arch Biochem Biophys* 2015; **584**: 10-19 [PMID: 26319175 DOI: 10.1016/j.abb.2015.08.013]
- 54 **Wang G**, Li W, Lu X, Zhao X. Riboflavin alleviates cardiac failure in Type I diabetic cardiomyopathy. *Heart Int* 2011; **6**: e21 [PMID: 22355488 DOI: 10.4081/hi.2011.e21]
- 55 **Badawy AA**. Kynurenine Pathway of Tryptophan Metabolism: Regulatory and Functional Aspects. *Int J Tryptophan Res* 2017; **10**: 1178646917691938 [PMID: 28469468 DOI: 10.1177/1178646917691938]
- 56 **Bae SJ**, Lee JS, Kim JM, Lee EK, Han YK, Kim HJ, Choi J, Ha YM, No JK, Kim YH, Yu BP, Chung HY. 5-Hydroxytryptophan inhibits tert-butylhydroperoxide (t-BHP)-induced oxidative damage via the suppression of reactive species (RS) and nuclear factor-kappaB (NF-kappaB) activation on human fibroblast. *J Agric Food Chem* 2010; **58**: 6387-6394 [PMID: 20415419 DOI: 10.1021/jf904201h]
- 57 **Cheng SC**, van de Veerdonk F, Smeeckens S, Joosten LA, van der Meer JW, Kullberg BJ, Netea MG. *Candida albicans* dampens host defense by downregulating IL-17 production. *J Immunol* 2010; **185**: 2450-2457 [PMID: 20624941 DOI: 10.4049/jimmunol.1000756]
- 58 **Ohgi Y**, Futamura T, Kikuchi T, Hashimoto K. Effects of antidepressants on alternations in serum cytokines and depressive-like behavior in mice after lipopolysaccharide administration. *Pharmacol Biochem Behav* 2013; **103**: 853-859 [PMID: 23262300 DOI: 10.1016/j.pbb.2013.05.003]

- 10.1016/j.pbb.2012.12.003]
- 59 **Abdala-Valencia H**, Berdnikovs S, McCary CA, Urick D, Mahadevia R, Marchese ME, Swartz K, Wright L, Mutlu GM, Cook-Mills JM. Inhibition of allergic inflammation by supplementation with 5-hydroxytryptophan. *Am J Physiol Lung Cell Mol Physiol* 2012; **303**: L642-L660 [PMID: 22842218 DOI: 10.1152/ajplung.00406.2011]
- 60 **Zhao H**, Chen S, Hu K, Zhang Z, Yan X, Gao H, Du W, Zheng H. 5-HTP decreases goat mammary epithelial cells apoptosis through MAPK/ERK/Bcl-3 pathway. *Gene* 2021; **769**: 145240 [PMID: 33068678 DOI: 10.1016/j.gene.2020.145240]
- 61 **Jiang J**, Yu S, Jiang Z, Liang C, Yu W, Li J, Du X, Wang H, Gao X, Wang X. N-acetyl-serotonin protects HepG2 cells from oxidative stress injury induced by hydrogen peroxide. *Oxid Med Cell Longev* 2014; **2014**: 310504 [PMID: 25013541 DOI: 10.1155/2014/310504]
- 62 **Zhao Y**, Wang H, Chen W, Chen L, Liu D, Wang X. Melatonin attenuates white matter damage after focal brain ischemia in rats by regulating the TLR4/NF-κB pathway. *Brain Res Bull* 2019; **150**: 168-178 [PMID: 31158461 DOI: 10.1016/j.brainresbull.2019.05.019]
- 63 **Favennec M**, Hennart B, Caiazza R, Leloire A, Yengo L, Verbanck M, Arredouani A, Marre M, Pigeyre M, Bessede A, Guillemin GJ, Chinetti G, Staels B, Pattou F, Balkau B, Allorge D, Froguel P, Poulain-Godefroy O. The kynurenine pathway is activated in human obesity and shifted toward kynurenine monooxygenase activation. *Obesity (Silver Spring)* 2015; **23**: 2066-2074 [PMID: 26347385 DOI: 10.1002/oby.21199]
- 64 **Oxenkrug G**. Insulin resistance and dysregulation of tryptophan-kynurenine and kynurenine-nicotinamide adenine dinucleotide metabolic pathways. *Mol Neurobiol* 2013; **48**: 294-301 [PMID: 23813101 DOI: 10.1007/s12035-013-8497-4]
- 65 **O'Neill LA**, Golenbock D, Bowie AG. The history of Toll-like receptors - redefining innate immunity. *Nat Rev Immunol* 2013; **13**: 453-460 [PMID: 23681101 DOI: 10.1038/nri3446]
- 66 **Wan RJ**, Li YH. Effects of Artesunate prevent nephritis via the Tolllike receptor 4/nuclear factorκB signaling pathway in rats. *Mol Med Rep* 2017; **16**: 6389-6395 [PMID: 28849172 DOI: 10.3892/mmr.2017.7362]
- 67 **Zhang C**, Boini KM, Xia M, Abais JM, Li X, Liu Q, Li PL. Activation of Nod-like receptor protein 3 inflammasomes turns on podocyte injury and glomerular sclerosis in hyperhomocysteinemia. *Hypertension* 2012; **60**: 154-162 [PMID: 22647887 DOI: 10.1161/HYPERTENSIONAHA.111.189688]
- 68 **Guo Z**, Yu S, Chen X, Ye R, Zhu W, Liu X. NLRP3 Is Involved in Ischemia/Reperfusion Injury. *CNS Neurol Disord Drug Targets* 2016; **15**: 699-712 [PMID: 26996163 DOI: 10.2174/1871527315666160321111829]
- 69 **Garibotto G**, Carta A, Picciotto D, Viazzi F, Verzola D. Toll-like receptor-4 signaling mediates inflammation and tissue injury in diabetic nephropathy. *J Nephrol* 2017; **30**: 719-727 [PMID: 28933050 DOI: 10.1007/s40620-017-0432-8]
- 70 **Wang F**, Liu C, Ren L, Li Y, Yang H, Yu Y, Xu W. Sanziguben polysaccharides improve diabetic nephropathy in mice by regulating gut microbiota to inhibit the TLR4/NF-κB/NLRP3 signalling pathway. *Pharm Biol* 2023; **61**: 427-436 [PMID: 36772833 DOI: 10.1080/13880209.2023.2174145]
- 71 **Kim EK**, Choi EJ. Pathological roles of MAPK signaling pathways in human diseases. *Biochim Biophys Acta* 2010; **1802**: 396-405 [PMID: 20079433 DOI: 10.1016/j.bbadis.2009.12.009]
- 72 **Ma FY**, Liu J, Nikolic-Paterson DJ. The role of stress-activated protein kinase signaling in renal pathophysiology. *Braz J Med Biol Res* 2009; **42**: 29-37 [PMID: 18982195 DOI: 10.1590/S0100-879X2008005000049]
- 73 **Wang X**, Li C, Huan Y, Cao H, Sun S, Lei L, Liu Q, Liu S, Ji W, Huang K, Shen Z, Zhou J. Diphenyl diselenide ameliorates diabetic nephropathy in streptozotocin-induced diabetic rats via suppressing oxidative stress and inflammation. *Chem Biol Interact* 2021; **338**: 109427 [PMID: 33639173 DOI: 10.1016/j.cbi.2021.109427]



Published by **Baishideng Publishing Group Inc**
7041 Koll Center Parkway, Suite 160, Pleasanton, CA 94566, USA
Telephone: +1-925-3991568
E-mail: office@baishideng.com
Help Desk: <https://www.f6publishing.com/helpdesk>
<https://www.wjgnet.com>

